LEVERAGING DISCRIMINATIVE DICTIONARY LEARNING ALGORITHMS FOR SINGLE LEAD ECG CLASSIFICATION

by

Sherin Mary Mathews

A thesis submitted to the Faculty of the University of Delaware in partial fulfillment of the requirements for the degree of Master of Science in Electrical and Computer Engineering

Spring 2015

LEVERAGING DISCRIMINATIVE DICTIONARY LEARNING ALGORITHMS FOR SINGLE LEAD ECG CLASSIFICATION

by

Sherin Mary Mathews

Approved: ____

Kenneth E. Barner, Ph.D.
Professor in charge of thesis on behalf of the Advisory Committee

Approved: ____

Kenneth E. Barner, Ph.D.
Chair of the Department of Electrical and Computer Engineering

Approved: ____

Babatunde Ogunnaike, Ph.D.
Dean of the College of Engineering

Approved: ____

James G. Richards, Ph.D.
Vice Provost for Graduate and Professional Education

TABLE OF CONTENTS

LIST OF TABLES

LIST OF FIGURES

ABSTRACT

Detecting and classifying cardiovascular diseases and their underlying etiology are necessary in critical-care patient monitoring. In this thesis, we explore the effectiveness of discriminative dictionary learning algorithms for electrocardiogram (ECG) classification task and exhibit that they can achieve very competitive performance compared to traditional methods with lower computational cost. We demonstrate dictionary learning and classification processes simultaneously following the detection of supraventricular and ventricular heartbeats using a single-lead ECG. Label information for each dictionary atom is incorporated to enforce discriminability in sparse codes during the dictionary-learning process. Such a discriminative label-consistent learning procedure for adapting both dictionaries and classifier to a specified ECG signal, rather than employing pre-defined dictionaries is novel.

The effectiveness of the proposed algorithms is demonstrated on real ECG signals from the MIT-BIH arrhythmia database. The performance of the algorithm is evaluated in terms of classification accuracy, sensitivity, positive predictive value and false positive ratio. The results demonstrate a classification accuracy of 94.61% for Supra Ventricular Ectopic Beats (SVEB) class and 97.18% for Ventricular Ectopic Beats (VEB) class at sampling rate of 114 Hz on MIT-BIH database. Therefore, a sampling rate of 114 Hz provided enough discriminatory power for the classification task. Results illustrated that our approach gave emulous results as compared to the state of the art models at a lower sampling rate and a set of simple features. Experimental results also illustrate a classification accuracy of 94.48% for SVEB class and 96.95% for VEB class at sampling rate of 360Hz, thereby indicating that our algorithm

is capable of achieving superior classification performance with substantially higher efficiency compared to the state of art methods in ECG classification.

Chapter 1

INTRODUCTION

1.1 Problem Formulation

Cardiac arrhythmias are abnormal heart rhythms that can cause a serious threat to the patients recovering from acute myocardial infarction [1]. Some types of arrhythmias are life-threatening medical emergencies that can trigger cardiac arrest and sudden death. Since ECG signals furnish valuable information about the electrophysiology of the heart diseases and functional aspects of the cardiovascular system, they are considered useful in diagnosing cardiac disorders and detecting any arrhythmia. Early automatic detection and classification of ECG patterns is therefore critical in diagnosis and treatment of patients with life-threatening cardiac arrhythmia [2], [3].

Several algorithms have focused on automatic classification of heartbeats, which gives valuable results taking advantage of easily recorded cardiac electrical signals. These methods, however, classify the arrhythmias at higher sampling rate and hence need a lot of computational time. It thus becomes necessary to enlarge classification criteria using a set of simple features and at lower sampling rate which would enable implementation in real time and at lower cost. This calls for a more accurate and robust which would report lesser false alarms, thereby making it clinically more practical.

Recent works have exhibited the benefits of applying sparse coding in computer vision and image classification [4], [5]. The objective of this thesis is to propose a novel sparse-based classification algorithm for ECG signals. The proposed algorithm demonstrates dictionary learning and classification processes simultaneously following the detection of supraventricular and ventricular heartbeats using a single-lead ECG. In addition to using class labels of training data, label information for each dictionary atom (the columns of the dictionary matrix) is incorporated to enforce discriminability in sparse codes during the dictionary-learning process. Experimental results indicate that classifiers built into this learning-based dictionary framework emulated performance of state-of-the -art models at a lower sampling rate (114 Hz), a rate found to provide sufficient discriminatory power for the classification task.

1.2 State of the Art

Accurate, noninvasive diagnosis of CVD has been a challenge for recent years and various methods have been proposed in the literature for detection and classification of ECG beats. Feature extraction methods explored to discriminate heartbeats include using wave shape [6], [7], [8], [9], [10], Hermite functions [11], wavelet-based features [12], [13], frequency-based features [14], ECG morphology [15], hermite polynomials [16], higher order cumulant features [17], statistical features [18], [19] and Karhunen-Loeve expansion of ECG morphology [15].

Classifiers methods employed include support vector machines [10], [20], [18], self organizing maps with learning vector quantisation [16], *k-th* nearest-neighbours rules [21], decision trees [20], artificial neural networks [22], linear discriminants [6], [7], [9], active learning framework [23] and back propagation neural networks [17]. Although several statistically motivated approaches have been proposed, to the best of our knowledge a dictionary-learning algorithm has not before been used for ECG classification tasks. As learning the dictionary from the training samples instead of using Fourier or wavelet bases has been effective for face recognition, we propose applying this technique to ECG classification [24]. Incorporating this discriminative learning procedure with simple features at lower sampling rate gives competitive classification performance at lower computational cost.

The discriminative learning procedure used here adapts the dictionaries to the specified task, instead of employing pre-defined dictionaries, and also finds the linear classifier parameters in the same procedure. To our knowledge, dictionary learning algorithm and also discriminative learning has not been used before for ECG classification tasks. The feature sets used in this experiment are more feasible as they are time based features derived at a lower sampling rate. This simple set of features at lower sampling rate gave enough discriminatory performance for classification which is more practical due to its lower computational cost.

1.3 Summary of Contributions

The main contributions of this thesis are as follows:

- By applying the discriminative dictionary learning algorithms to electrocardiogram signal recognition, we first introduce this emerging technique into biomedical signal classification.

- More importantly, we show that dictionary learning algorithm demonstrates the promising performance compared to human-engineered algorithms at a lower sampling rate of 114 Hz.

- The algorithm was also able to provide competitive classification performance compared to state of art methods at a sampling rate of 360 Hz.

1.4 Related Publication to The Described Contributions

The contributions described in this thesis appeared in the following publication.

- Sherin M. Mathews, Luisa F. Polania and Kenneth E. Barner, "Leveraging a discriminative dictionary learning algorithm for single-lead ECG classification ", at *Northeast Bioengineering Conference (NEBEC)*, April 2015.

Chapter 2

DICTIONARY LEARNING BACKGROUND

2.1 Sparse Representation and Dictionary Learning

Sparse coding finds applications in varied problems in computer vision *i.e.,* image classifciation, image denoising [25], image restoration [26], [27]. A sparse signal can be summarily expressed as a linear combination of a few signal items (called atoms or bases) from an over-complete dictionary. While sparse representation needs compact linear combinations of atoms from a given dictionary, dictionary learning intents to adapt the dictionary to better fit the task-specific model [28]. Strictly speaking, for a large set of training signals, dictionary learning needs a succinct set of atoms to best characterize each signal in the training set under defined sparsity constraints. Dictionary learning problem can be formulated as follows:

Let $\mathbf{Y}$ be a set of n-dimensional N input signals $\mathbf{Y} = [\mathbf{y}_1, \mathbf{y}_2, \ldots, \mathbf{y}_N] \in \mathbb{R}^{n \times N}$. A dictionary $\mathbf{D}$ to sparsely represent $\mathbf{Y}$ and corresponding sparse codes $\mathbf{X} = [\mathbf{x}_1, \ldots, \mathbf{x}_N]$ are learned by solving the optimization problem

$$< \mathbf{D}, \mathbf{X} >= \arg\min_{\mathbf{D},\mathbf{X}} \|\mathbf{Y} - \mathbf{DX}\|_2^2 \,, \quad \text{s.t.} \forall_i, \|x_i\|_0 \leq T \tag{2.1}$$

where $\mathbf{T}$ is sparsity constraint factor. Because a good classifier can be obtained by determining the parameters, model parameters $\mathbf{W}$ and dictionary $\mathbf{D}$ can be jointly learned by

$$< \mathbf{D}, \mathbf{W}, \mathbf{X} >= \arg\min_{\mathbf{D},\mathbf{W},\mathbf{X}} (\|\mathbf{Y} - \mathbf{DX}\|_2^2 + \sum_i \mathcal{L}\{h_i, f(x_i, W)\} + \lambda_1 \|\mathbf{W}\|_F^2), \text{s.t.} \forall_i, \|x_i\|_0 \leq T \tag{2.2}$$

where $\mathcal{L}$ is a classification loss function, h_i is label of y_i and λ_1 is a regularization parameter.

A typical technique to minimize the above objective is by iteratively solving for sparse representations based on the dictionary and updating the dictionary given the sparse codes, until the constraint is met.

2.2 Motivation and Significance of Dictionary Learning and Sparse Representation in ECG Classification

An ECG signal rhythm can be determined by knowing the classification of consecutive heartbeats in the signal. Classifying ECG arrhythmia is quite a challenging task as arrhythmias appear as sequences of heartbeats with unusual timing and wave shape. Early automatic, precise detection and classification of the beats is hence critical in diagnosis and treatment of patients with life-threatening cardiac arrhythmia as it causes a serious threat to the patients recovering from acute myocardial infarction.

Several automatic arrhythmia detection procedures were developed in last ten years, owing to need of intensive care units for permanent monitoring of the patients. Existing methods reach good results but furnish only limited information about a signal by ignoring its hidden nonlinear dynamics and also requires more computational time It therefore becomes essential to enlarge classification approach by using a smaller set of features and novel algorithms for classification of arrhythmias to enable real time implementation [29].

Particularly due to its robustness to missing data and noise, dictionary learning has been successfully applied to many problems namely infilling missing pixels, image and speech classification problems. However, little efforts have been made to ECG classification using this model. It is thus desirable to exploit the capability of dictionary learning for robust arrthymia classification.

In comparison to the state of the art in ECG classification, the most important novelty of the proposed algorithm is use of dictionary learning algorithm for classification. The discriminative learning procedure used here adapts the dictionaries to the specified task, instead of employing pre-defined dictionaries, and also the linear classifier parameters in the same procedure. Incorporating this discriminative learning procedure with simple features at lower sampling rate gives competitive classification performance at lower computational cost. The feature sets used in this experiment are real time-based as they are time based features derived at a lower sampling rate. This simple set of features at lower sampling rate gave enough discriminatory performance for classification which seems more practical due to its lower computational cost.

To our knowledge, dictionary learning algorithm and also discriminative learning has not been used before for ECG classification tasks. Benefits of the proposed algorithm are two fold. First due to the use of a simpler set of features, it has lower computational cost thereby allowing real-time implementation on a power limited devices such as Holter ECG recorders. In addition, the proposed discriminative dictionary learning algorithm opens a new window for future research, showcasing the dictionary learning based methods provide huge potential for accurate ECG data classification.

2.3 State of the Art Algorithms in Dictionary Learning

To scale to large datasets, many dictionary learning (DL) algorithms have been developed to learn a compact dictionary. Training samples can be manually elected to formulate the dictionary, whereas a separate dictionary can be learned for each class with classification being performed based on reconstruction error. In Wright [5], all training samples of all classes was used as the dictionary to code for query image, and classification decision was based by evaluating which class leads to the minimal reconstruction error. Construction of dictionary during training and sparse coding during testing thereby became typically time consuming for large number of classes.

K-SVD [28] is one of the forefront dictionary learning algorithms, which focuses on the best sparse representation for the training signals of the learned dictionary, but does not consider the discrimination capability of the dictionary. The optimization here is an iterative process shifting between solving sparse representations using Orthogonal Matching Pursuit (OMP) and updating the dictionary using singular value decomposition (SVD). Method of optimal directions (MOD) [30] heritages the same sparse coding as K-SVD, wherein it employs either Orthogonal Matching Pursuit (OMP) or FOCUSS to solve for sparse codes and updates the dictionary effectively during learning. In [31], the dictionary and classifier learning methodology was combined to obtain Discriminative K-SVD algorithm .

There are approaches that aim to minimize the residual error of reconstructing the original signals without utilizing the class information in the training set. Such techniques are referred as unsupervised dictionary learning; dictionaries learned in such a fashion can be used for classification tasks; examples include [4], [5], [32]. Recent research [31], [33] , [34] , [35] reveal that dictionaries formulated using supervised learning resulted in improved classification performances and hence we leverage a supervised algorithm to learn a compact and discriminative dictionary for sparse coding for ECG arrthymia classification.

Chapter 3

PROPOSED METHODOLOGY

3.1 Salient Characteristics of an ECG Signal

3.1.1 ECG wave, segments and intervals

An ECG signal furnishes valuable information about the electrophysiology of the heart diseases and functional condition of the cardiovascular system. As the state of cardiac heart generally reflects in the shape of ECG waveform, an ECG waveform is considered to be a quintessential signal of cardiac physiology, helpful in diagnosing cardiac disorders and detecting any arrhythmia. An ECG wave consists of positive deflections (peaks) and negative deflections (formations) which makes it symbolic in diagnosis. A cardiac cycle of a typical heartbeat has a distinctive structure represented by the P-QRS-T wave form as seen in Fig. 3.1 and described as follows:

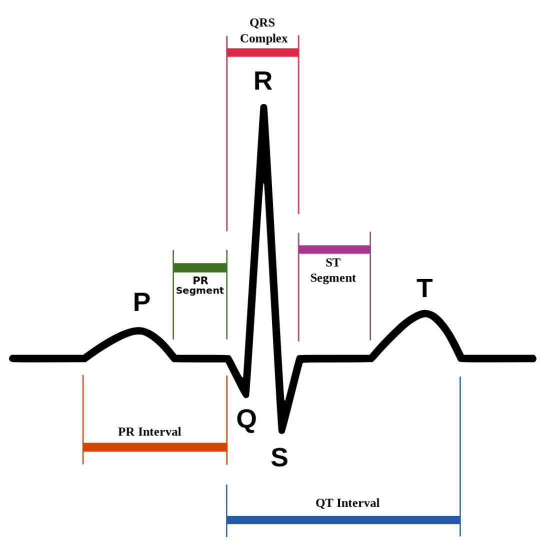

Figure 3.1: ECG cardiac cycle represented by the P-QRS-T wave form [36]

- **P-wave** - represents atrial depolarization wherein blood flows from atria to ventricles [37].
- **Q wave** - represents the normal left-to-right depolarisation of the interventricular septum .
- **R wave** - represents early depolarization of the ventricle as it epitomize the electrical stimulus which passes through the main portion of the ventricular walls .
- **S wave** - represents final depolarization of the ventricles .
- **T wave** - represents electrical repolarization (recovery) of the ventricles .
- **PR segment** - represents isoelectric segment between the end of the P wave and the start of the QRS complex. It corresponds to the time between the end of atrial depolarization to the outset of ventricular depolarization .
- **QRS complex** - represents ventricular depolarization which thereby triggers contraction of the ventricles. QRS corresponds to simultaneous activation of the right and left ventricles .
- **S-T segment** - represents the interval between ventricular depolarization and repolarization. It corresponds to the time from the offset of the QRS complex to onset of the T wave .
- **PR interval** - represents the conduction through the AV node. It corresponds to the time needed for an electrical impulse to travel from the sinus node through the AV node and thereafter entering the ventricles .
- **Q-T interval** - represents the time from the onset of the Q wave to the offset of the T wave. It corresponds to the time taken for both ventricular depolarisation and repolarisation, and therefore roughly estimates the duration of an average ventricular action potential .

3.2 Noise in ECG Signal

An ECG signal is usually corrupted by different types of artifacts and noise which lie within the frequency band of ECG signal. These artifacts alter the characteristics of ECG signal making it difficult to extract purposive information from the signal.

The corruption of ECG signal is due to following major noises:

- Base-line drift : Base-line drift is caused in chest-lead ECG signals due to coughing or breathing, or when an arm or leg is moved during limb-lead ECG acquisition.

- Power line interference : Power line interference is caused due to improper grounding and is indicated as an impulse at 50 Hz/60 Hz harmonics. It also appears as additional spikes at integral multiples of the fundamental frequency.

- Motion artifacts : Motion artifacts are transient baseline change due to electrode skin impedance with electrode motion.

Filtering of artifacts and noise is very crucial in the investigation of biomedical signals, particularly in the case of signals as weak as the electrocardiogram. Methods of noise reduction have influential effect on performance of all ECG signal processing systems.

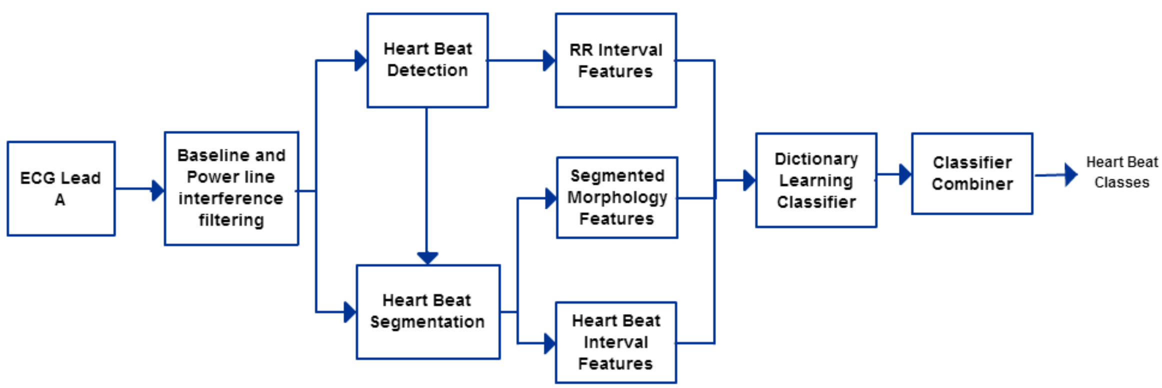

Figure 3.2: Outline of the Entire Process

3.3 Preprocessing

Each ECG signal is bandpass filtered at 0.110 Hz and sampled at 360 Hz. Preprocessing forms the first stage in the entire procedure where it utilizes a filtering unit to remove artifact signal, i.e. baseline wander, power line interference and high frequency noise, using the method enumerated in [6]. This section describes different types of ECG artifacts and the relevant preprocessing technique used to remove these artifacts.

3.3.1 Base-line drift

Baseline wander is a low frequency artifact in ECG signal may be caused in chest-lead ECG signals by coughing or breathing with large movement of the chest, electrode skin contact or when an arm or leg is moved in the case of limb-lead ECG acquisition [6]. Eliminating this kind of artifact therefore becomes a primary step in ECG signal processing before using it for accurate further diagnostic purpose.

To remove baseline wander, we pass the signal through median filters of window sizes 200ms and 600ms. This removes P-waves, QRS complexes and T-waves leaving behind the baseline wander. By subtracting the baseline wander from the original signal, we obtained the filtered signal.

3.3.2 Power line interference

Power line interference is symbolized as a 50 Hz frequency impulse and appears as additional spikes at integral multiples of the fundamental frequency. Power line interference is effortlessly observable as the interfering voltage that might completely obscure the ECG waveform with frequencies in integral multiples of 50 Hz. This strong interference can be due to improper grounding, loose contacts with patients cable as well as disconnected electrodes. These transients can also be introduced by an electrical power systems inducing a rapid pulse on the trace due to switching action. Poor quality tracings obtained due to electromagnetic interference from the power lines thereby makes it crucial to suppress these transients. The power-line interference and high-frequency noise is removed from the baseline corrected ECG using a 12-tap low-pass filter. The filter is a finite impulse response filter with equal ripple in the pass and stop bands having 3-dB point at 35 Hz [15].

3.3.3 Motion artifacts

Motion artifacts are transient baseline interference introduced due to electrode skin impedance with electrode motion. Specifically, the electrode motion causes deformations of the skin around the electrode site, which in turn results in variations in the electrical characteristics of the skin around the electrode. It can result in larger amplitude signal in ECG waveform The peak amplitude of motion artifact is 500 percent of Peak to Peak ECG amplitude and the duration is about 100-500 ms Motion artifact can thus obscure the ECG waveforms making ECG interpretation quite difficult. An adaptive filter is used to remove the interference of motion artifacts.

3.4 Feature Extraction Methodology

A pattern recognition system aims to demonstrate a framework that automatically maps an input signal to a class label it belongs, by analyzing the features extracted from the signal. The two symbolic stages of a pattern recognition system include feature extraction and classification. Prior to feature extraction, the data is processed i.e it is filtered followed by detection and segmentation. Thereafter, feature extraction employs mathematical techniques on input signal to build an association with known models and also obtain the best discriminative representation of the data by exploiting the underlying signal characteristics. The detailed technique used in each stage is enumerated as follows:

3.4.1 Detection and Segmentation

The processing stage consists of heartbeat detection and segmentation modules. For detection, the manually verified heartbeat fiducial point times provided with the MIT-BIH arrhythmia database were utilized [38]. Heartbeat segmentation program of Laguna [6] was used, since the the accuracy of the system in determining heartbeat segmentation points has been validated on the MIT-BIH database and has proved to be commensurate with the interexpert variation. Heartbeat segmentation stage provides QRS onset, offset and T-wave offset times; a Boolean value indicating the presence absence of a P-wave and, if present, it gave the P-wave onset and offset time for each heartbeat fiducial point.

3.4.2 Feature Extraction

Post the processing, the two feature sets (feature set 1 (FS1) and feature set 2 (FS2) are calculated. We settled for the single lead feature extraction method after it was found that, having more sample values in the feature vector do not produce significant improvement in performance [8]. It is noted that a lower sampling rate and smaller feature vector is quite desirable in real time monitoring applications as it translates to lesser power consumption and lower hardware complexity.

3.4.2.1 Feature Set 1

Feature Set 1 (FS1) consited of 26 features comprising of RR intervals, heartbeat intervals and segmented morphology [6] .(see Figure 3.3)

Intervals Features

RR-intervals also known as "Heartbeat fiducial point intervals" correspond to the interval between successive heartbeat fiducial points. The following four features were extracted from RR-intervals:

- **Pre-RR-interval** - is the RR-interval between a given heartbeat and the preceding heartbeat.
- **Post-RR-interval** - is the RR-interval between a given heartbeat and the next heartbeat.
- **Average RR-interval** - is the mean of RR-intervals for a recording. This value remains the same for all heartbeats in a recording.
- **Local average RR-interval** - is estimated by averaging RR-intervals of ten RR-intervals surrounding a heartbeat.

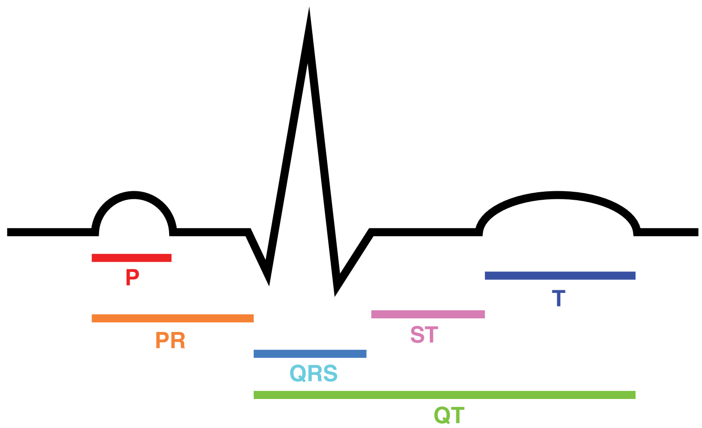

Figure 3.3: ECG Cardiac Trace [39]

Heart-beat Intervals Features

Three features were extracted from heart-beat intervals post heartbeat segmentation. (see Figure 3.3)

- **QRS duration** - is time interval between the QRS onset and QRS offset.
- **T-wave duration** - is time interval between QRS offset and T-wave offset.
- **Boolean variable** - is the third variable which indicates the presence or absence of a P-wave.

Segmented Morphology Intervals Features

Segmented morphology encompasses amplitude values of the ECG signal calculated by a sampling window between QRS onset and offset and a sampling window between QRS offset and T-wave offset points. Post the determination of fiducial point (FP), two sampling windows were utilized. The first window was bounded by the QRS onset and offset. The boundaries for the second window was determined by the QRS offset and the T-wave offset. Ten evenly spaced sample features were derived by uniformly sampling the ECG amplitude in the first window (Figure 3.4) and nine features were derived by uniformly sampling the second window resulting in a total of 19 features [6](Figure 3.4).

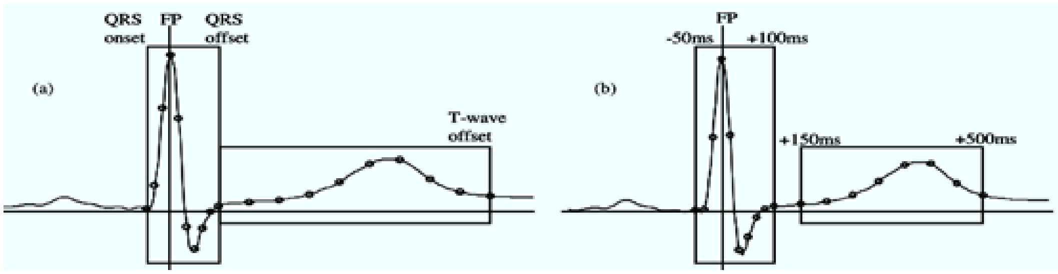

Figure 3.4: Segmented Morphology Intervals Features [6]

3.4.2.2 Feature Set 2

Feature Set 2 (FS2) has 22 features which consisted of RR intervals and fixed interval morphology [6].

RR Intervals Features

RR-intervals also known as "Heartbeat fiducial point intervals " correspond to the interval between successive heartbeat fiducial points. These are the same four features that were extracted in Feature Set 1.

Fixed interval morphology Features

To determine the fixed interval morphology features, the sampling windows were first positioned at the heartbeat fiducial point (FP). Two sampling windows were formed based on FP. The first window approximately encompassed the QRS-complex and covered the portion of the ECG between FP-50 ms and 100 ms. Nine samples of the ECG between FP-50ms and FP+100ms were extracted from this window. The second window approximately covered the T-wave and started at 150 ms and finished at 500 ms . The next nine samples between FP+150ms and FP+500ms are extracted from the second window. Therefore a total of 18 features were used in Feature Set 2.

Therefore the entire feature extraction can be summarized as:

- **Feature Set 1** (26) : RR intervals(4), Heart-beat intervals(3), Segmented Morphology(19)
- **Feature Set 2** (22) : RR intervals(4), Fixed Interval Morphology (18)

3.5 Classification Methodology using Label Consistent Dictionary Learning

The label consistent discriminative dictionary learning algorithm aims to leverage the supervised label information of input signals inorder to learn a compact discriminative dictionary for sparse coding. It embodies a discriminative sparse coding error criterion and an optimal classification performance criterion into the objective function which is optimized using K-SVD algorithm. The learned dictionary is therefore both discriminative and reconstructive, in contrast to traditional constructive ones [5], [28], [30]. The algorithm performs better by using a simple multiclass linear classifier, in contrast to other existing approaches [31], [40], [41] which learn one classifier for each pair of categories and [42], [43] which learn the dictionary and classifier separately .

To maintain explicit association between dictionary items and the labels, each dictionary item is chosen such that it represents a subset of the training signals from a single class, so each dictionary item corresponds to its particular label. The algorithm is targeted on the effects of adding a label consistency regularization term and a joint classification error into the objective function in for learning the dictionary. These are referred as LC-KSVD1 and LC-KSVD2, respectively, as explained in the following.

3.5.1 Label Consistent KSVD 1 (LCKSVD 1)

The classification algorithm explicitly incorporates a label consistency constraint called "discriminative sparse-code error" and an optimal classification performance criteria into the objective function and optimizes it using the K-SVD algorithm. In addition to using class labels of training data, label information with each dictionary item (columns of the dictionary matrix) is used to enforce discriminability in sparse codes during the dictionary learning process. Thus, the learned dictionary enables the signals from the same class to have identical sparse codes and signals from different classes to have non- identical sparse codes, thereby enabling to achieve good accuracy even with a simple multiclass linear classifier.

For obtaining discriminative sparse codes $\mathbf{Q}$, for an input training signal $\mathbf{Y}$ with learned $\mathbf{D}$, the objective function for **Label Consistent KSVD 1 (LCKSVD1)** can be defined as

$$< \mathbf{D}, \mathbf{A}, \mathbf{X} >= \underset{\mathbf{D},\mathbf{A},\mathbf{X}}{\arg\min}(\|\mathbf{Y} - \mathbf{DX}\|_2^2 + \alpha \, \|\mathbf{Q} - \mathbf{AX}\|_2^2)\text{s.t. } \forall_i, \|x_i\|_0 \leq T \tag{3.1}$$

where A is a linear transformation matrix and α is the scalars controlling the relative contribution between reconstruction and label consistency regularization. Here, the linear transformation *g (x; A)=Ax* converts the sparse codes $\mathbf{x}$ to be the most discriminative in sparse feature space and hence the term $\|\mathbf{Q} - \mathbf{AX}\|_2^2$ corresponds to the discriminative sparse code error. Discriminative sparse code error compels the signals of the same class to have identical sparse representations thereby resulting in good classification performance by using just a simple linear classifier.

3.5.2 Label Consistent KSVD 2 (LCKSVD 2)

For Label Consistent KSVD 2 (LCKSVD2), the classification error term is included in order to make the dictionary optimal for classification. Considering a linear-predictive classifier *f (x; W)=Wx* , the objective function for learning a dictionary D can be defined as

$$< \mathbf{D}, \mathbf{W}, \mathbf{X} >= \underset{\mathbf{D},\mathbf{W},\mathbf{X}}{\arg\min}(\|\mathbf{Y} - \mathbf{DX}\|_2^2 + \alpha \; \|\mathbf{Q} - \mathbf{AX}\|_2^2 + \beta \, \|\mathbf{H} - \mathbf{WX}\|_2^2 \,) \text{ s.t. } \forall_i, \|x_i\|_0 \leq T \tag{3.2}$$

where $H = [h_1, h_2, \ldots, h_N]$ are the class labels of input signals Y and α, β are the scalars controlling the relative contribution of the corresponding terms.

Here, the first term corresponds to the reconstruction error, the second one represents discriminative sparse-code error, and the third term corresponds to the classification error.

The objective function can be rewritten as

$$\left\| \begin{bmatrix} \mathbf{Y} \\ \sqrt{\alpha}\mathbf{Q} \\ \sqrt{\beta}\mathbf{H} \end{bmatrix} - \begin{bmatrix} \mathbf{D} \\ \sqrt{\alpha}\mathbf{A} \\ \sqrt{\beta}\mathbf{W} \end{bmatrix} \mathbf{X} \right\|_2^2 \tag{3.3}$$

Let $\mathbf{Y_{new}} = (\mathbf{Y^t}, \sqrt{\alpha}\mathbf{Q^t}, \sqrt{\beta}\mathbf{H^t})^t$ and $\mathbf{D_{new}} = (\mathbf{D^t}, \sqrt{\alpha}\mathbf{A^t}, \sqrt{\beta}\mathbf{W^t})^t$ therefore the optimization of eq 3.3 becomes proportionate to solving :

$$< \mathbf{D_{new}}, \mathbf{X} >= \underset{\mathbf{D_{new}}, \mathbf{X}}{\arg\min} (\|\mathbf{Y_{new}} - \mathbf{D_{new}}\mathbf{X}\|_2^2) \quad \text{s.t. } \forall_i, \|x_i\|_0 \le T \tag{3.4}$$

This equation can be solved by using KSVD, thereby making the learned dictionary both reconstructive and discriminative, in contrast to traditional purely constructive ones. Applying KSVD gives us $D = [d_1, \ldots, d_K]$ and $W = [w_1, \ldots, w_K]$. However matrices $\mathbf{D}$, $\mathbf{A}$, and $\mathbf{W}$ cannot be directly used, as they are ℓ_2-normalized. The desired dictionary $\hat{\mathbf{D}}$, transform parameters $\hat{\mathbf{A}}$, and classifier parameters $\hat{\mathbf{W}}$ are therefore computed as in [24].

$$\hat{D} = [d_1/\|d_1\|_2 \ \ldots d_k/\|d_k\|_2 \ ] \tag{3.5}$$

$$\hat{A} = [a_1/\|d_1\|_2 \ \ldots a_k/\|d_k\|_2 \ ] \tag{3.6}$$

$$\hat{W} = [w_1/\|d_1\|_2 \ \ldots w_k/\|d_k\|_2 \ ] \tag{3.7}$$

This regression-based classification scheme only involving matrix multiplication is more efficient than other approaches that first must map computed sparse coefficients to each class and then use the reconstruction error for classification.

For testing data vector y_i, we first compute the sparse representation x_i by using orthogonal matching pursuit algorithm to solve the problem

$$\mathbf{x}_i = \underset{x_i}{\arg\min} \|y_i - \hat{\mathbf{D}}\mathbf{x}_i\|_2^2 \text{ s.t. } \forall_i, \|x_i\|_0 \le T \tag{3.8}$$

Thereafter using the linear predictive classifier $\hat{\mathbf{W}}$, we estimate the label j of the vector y_i

$$j = \arg\max_{j} \ (\hat{\mathbf{W}}_{j\cdot}\mathbf{x}_i) \ \text{ s.t. } \ \|x_i\|_0 \leq T \tag{3.9}$$

where $\hat{W}_{j\cdot}$ denotes the j th row of $\hat{W}$

In contrast to most existing dictionary learning approaches that reckon on iteratively solving sub-problems to approximate a global solution, the label consistent dictionary learning approach is able to learn the single compact dictionary, discriminative coding parameters and classifier parameters and the universal multiclass linear classifier simultaneously.

Chapter 4

EVALUATION OF PROPOSED METHODOLOGY

4.1 MIT - BIH Database

For the evaluation experiments, we used the acclaimed MIT/Beth Israel Hospital (BIH) Arrhythmia Database available at MIT medical data storage Physionet [38]:

Briefly, MIT-BIH Arrhytmia database [38] incorporates 48 half-hour ECG recordings, each containing two ECG lead signals digitized at 360 samples per second with 11-bit resolution over 10 mV range. Twenty-three recordings were randomly selected from a set of 4,000 24 hour ambulatory ECG data collected from a mixed population including both inpatients and outpatients at the medical center. The remaining 25 recordings were selected from the same set to include less common but clinically symbolic arrhythmias. All recordings have been annotated by two or more cardiologists and contain modified limb lead II. Second lead is usually modified lead V1, occasionally V2 or V5 and in one instance V4. In our experiment, we focused on using lead A only. In 45 recordings, lead A is modified lead II and for the other three is lead V5 [8]. According to the AAMI recommended practice, the 4 paced beats are excluded in this experimental evaluation process for the reason that these beats do not possess sufficient signal quality for reliable processing [6], [7].

4.2 AAMI Standard

MIT-BIH heartbeat types are combined according to Association for the Advancement of Medical Instrumentation (AAMI) recommendation. AAMI standard emphasize the problem of classifying ventricular ectopic beats (VEBs) from the non- ventricular ectopic beats . The normal and arrhythmia beats are remapped to the five

Remapped Classes	Classes Mapped in accordance to AAMI Standard				
Class N	Normal Beat (NOR)	Left Bundle Branch Block (LBBB)	Right Bundle Branch Block (RBBB)	Atrial Escape Beat (AE)	Nodal Escape Beat (NE)
Class S	Atrial Premature beat (AP)	Aberrated atrial premature beat (aAP)	supra ventricular premature beat (SP)	Nodal premature beat (NP)	
Class V	Premature Ventricular contraction (PVC)	Ventricular escape beat (VE)			
Class F	Fusion of normal & ventricular beat (Fvn)				
Class Q	paced beat (P)	Fusion of paced & normal beat (fPN)	unclassified beat (U)		

Table 4.1: MIT-BIH arrhythmia database heartbeat mapped to AAMI heartbeat classes

AAMI heartbeat classes using the mapping in [6]. Each class includes heartbeats of one or more types as shown in Table (6.1). The AAMI recommended practice was used to combine the MIT-BIH heartbeat types into following five heartbeat classes which were used in all subsequent processing.

1. Class N corresponding to beats originating in the sinus node (normal and bundle branch block beat types),
2. Class S corresponding to supraventricular ectopic beats (SVEBs),
3. Class V corresponding to ventricular ectopic beats (VEBs),
4. Class F corresponding to beats that result from fusing normal and VEBs,

5. Class Q corresponding to unknown beats including paced beats

4.3 Evaluation Metrics

The MIT -BIH database containing a series of manually verified QRS detection points is utilized in this study. After the four recordings containing paced beats were removed as in [7], the remaining 44 recordings were divided into two equal-sized datasets containing ECG data from 22 recordings. The first dataset (DS1) was used to train the classifier and to set parameters values for optimizing performance of the classifier. The second dataset (DS2) is employed for an independent and unbiased performance evaluation of the heartbeat classification system (see Fig. 4.1).

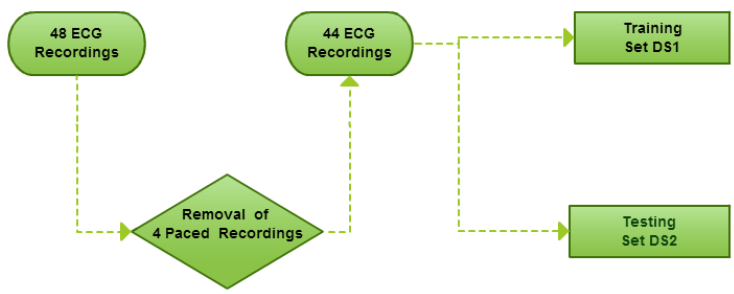

Figure 4.1: MIT-BIH database division into training and testing sets

For the validation of the algorithms on the MIT-BIH database ,the following performance metrics were used : accuracy (Acc), sensitivity (Se), positive predictive value (PPV), and false positive rate (FPR).

$$Accuracy(ACC) = \frac{TP + TN}{TP + TN + FP + FN} \tag{4.1}$$

$$Sensitivity(Se) = \frac{TP}{TP + FN} \tag{4.2}$$

$$PositivePredictiveValue(PPV) = \frac{TP}{TP + FP} \tag{4.3}$$

$$FalsePositiveRate(FPR) = \frac{FP}{TN + FP} \tag{4.4}$$

where TP is the true positive which corresponds to the number of heartbeats belonging to particular class A that are accurately classified to same class; FN is false negative which corresponds to the number of heartbeats belonging to particular class A that are inaccurately classified to differnt class B; FP is false positive which corresponds to the number of heartbeats belonging to class B that are inaccurately classified to class A; TN is true negative which corresponds to the number of heartbeats belonging to class B that are accurately classified to same class B.

4.4 Experimental Results and Discussion

Classification was performed on extensively used MIT-BIH arrhythmia database [38] to detect two types of heartbeat arrhythmias Ventricular Ectopic Beats (VEB) and Supra Ventricular Ectopic Beats (SVEB). In agreement with the AAMI recommended practice, four recordings containing paced beats were removed from 48 recordings and the data from 44 recordings were divided into two sets training (DS1) and test data (DS2). Classifier training was achieved using DS1 and performance assessment was determined using DS2. We have reported the ECG classification results at sampling rate of 360 Hz in tables 4.2 - 4.10 .

Record number	Beats Belonging to Class N	Beats Belonging to Class S	Beats Belonging to Class V	Beats Belonging to Class F	Beats Belonging to Class Q	Total Beats in Each Record
100	2252	14	7	0	0	2273
103	2056	26	2	0	0	2084
105	2241	87	206	38	0	2572
111	2101	16	7	0	0	2124
113	1638	118	39	0	0	1795
117	1512	23	0	0	0	1535
121	1710	145	8	0	0	1863
123	1289	229	0	0	0	1518
200	1660	118	775	48	0	2601
202	1274	804	54	4	0	2136
210	1424	117	1005	104	0	2650
212	2712	30	6	0	0	2748
213	2844	9	310	88	0	3251
214	1734	38	392	98	0	2262
219	1538	77	448	91	0	2154
221	1589	171	412	255	0	2427
222	1620	723	135	5	0	2483
228	1544	82	330	97	0	2053
231	1563	8	0	0	0	1571
232	439	1165	173	3	0	1780
233	1332	50	1145	552	0	3079
234	2688	47	13	5	0	2753

Table 4.2: Classification results per record for FS1 + LCKSVD at sampling rate of 360 Hz

Reference/Algorithm	N	S	V	F	Q
N	38123	2502	2367	1267	0
S	142	1384	303	8	0
V	187	210	2727	97	0
F	307	0	66	15	0
Q	1	1	4	1	0

Table 4.3: Classification results for FS 1 + LCKSVD at sampling rate of 360Hz

In accordance with AAMI recommendations, the classification performance for each recording and the gross performance figures were calculated using either feature set 1 or feature set 2 for feature extraction and label consistent discriminative dictionary learning algorithm at 360 Hz. Table 4.2 reports the gross classification performance

Record number	Beats Belonging to Class N	Beats Belonging to Class S	Beats Belonging to Class V	Beats Belonging to Class F	Beats Belonging to Class Q	Total Beats in Each Record
100	2236	36	1	0	0	2273
103	2067	17	0	0	0	2084
105	2391	64	96	21	0	2572
111	2108	10	6	0	0	2124
113	1631	153	11	0	0	1795
117	1473	62	0	0	0	1535
121	1849	12	2	0	0	1863
123	1477	41	0	0	0	1518
200	1972	70	558	1	0	2601
202	1468	607	53	8	0	2136
210	2401	60	188	1	0	2650
212	2712	26	10	0	0	2748
213	2961	10	261	19	0	3251
214	1940	45	250	27	0	2262
219	1870	162	121	1	0	2154
221	1827	74	413	113	0	2427
222	1626	785	71	1	0	2483
228	1653	59	341	0	0	2053
231	1557	12	1	1	0	1571
232	402	1013	365	0	0	1780
233	2224	26	702	127	0	3079
234	2707	38	3	5	0	2753

Table 4.4: Comparsion of classification results for FS2 + LCKSVD at sampling rate of 360 Hz

Reference/Algorithm	N	S	V	F	Q
N	41534	2048	362	315	0
S	108	1239	485	5	0
V	566	94	2556	5	0
F	341	0	47	0	0
Q	3	1	3	0	0

Table 4.5: Classification results for FS2 + LCKSVD at sampling rate of 360 Hz

for each recording using feature Set 1 and LCKSVD algorithm at a sampling rate of 360Hz; table 4.3 reports the per class classification performance for each defined AAMI class using feature Set 1 and LCSKVD algorithm at a sampling rate of 360Hz. Table

Reference/Algorithm	N	S	V	F	Q
N	86.13%	5.65%	5.34%	2.86%	0%
S	7.72%	75.34%	16.49%	0.43%	0%
V	5.80%	6.51%	84.66%	3.01%	0%
F	79.12%	0%	17.01%	3.86%	0%
Q	14.28%	14.28%	57.14%	14.28%	0%

Table 4.6: Classification results in % for FS 1 + LCKSVD at sampling rate of 360Hz

Reference/Algorithm	N	S	V	F	Q
N	93.84%	4.62%	0.81%	0.71%	0%
S	5.87%	67.44%	26.40%	0.27%	0%
V	17.57%	2.91%	79.35%	0.15%	0%
F	87.88%	0%	12.11%	0%	0%
Q	42.85%	14.28%	42.85%	0%	0%

Table 4.7: Classification results in % for FS 2 + LCKSVD at sampling rate of 360Hz

4.4 reports the gross classification performance for each recording using feature Set 2 and LCKSVD at a sampling rate of 360Hz; table 4.5 reported the per class classification performance for each defined AAMI class using feature Set 2 and LCSKVD algorithm at a sampling rate of 360Hz. The predicted per class classification results using algorithms FS1 - LCKSVD and FS2 - LCKSVD in table 4.3 and table 4.5 are reported in percentiles (%) in table 4.6 and 4.7. Classification results observed in table 4.2 and table 4.4 are satisfactory when compared to the per record classification results in [6]. Table 4.5 reports the complete per class classification performance for each defined AAMI class using Feature Set 2 and LCSKVD algorithm at a sampling rate of 360Hz. The gross classification performance per class indicates the number of classes that are misclassified. In table 4.3, 2502 normal (N) beats were misclassified as SVEB (S) beats, and, 1267 N beats were misclassified as fusion (F) beats. Likewise in table 4.5, 2048 normal (N) beats were misclassifed as SVEB (S) beats, and 315 N beats were misclassified as fusion (F) beats. As compared to results in [6], the number of misclassified heartbeats are reduced. Therefore, the results give competitive performance as compared to state of art algorithm [6] and [8]. Tables 4.8 and 4.9 illustrates the accuracy over the five remapped classes using FS1 and LCKSVD and FS2 and LCKSVD methodology at sampling rate of 360 Hz.

Classes	Class N	Class S	Class V	Class F	Class Q
Acc %	86.37%	93.63%	93.62%	96.48%	99.99%

Table 4.8: Accuracy for all classes using FS 1 + LCKSVD at sampling rate of 360Hz

Classes	Class N	Class S	Class V	Class F	Class Q
Acc %	92.47%	94.48%	96.95%	98.56%	99.99%

Table 4.9: Accuracy for all classes using FS 2 + LCKSVD at sampling rate of 360Hz

Method	Rate	SVEB				VEB			
	(Hz)	Acc	Se	PPV	FPR	Acc	Se	PPV	FPR
FS1+LCKSVD	360	93.63	75.34	33.78	5.66	93.62	84.66	50.52	5.75
FS2+LCKSVD	360	94.48	67.44	36.64	4.47	96.95	79.35	75.11	1.81
Chazel et al [6]	360	94.6	75.9	38.5	4.7	97.4	77.7	81.9	1.2
Chazel et al [8]	360	93.6	61.2	31.2	5.2	95.4	72.4	62.3	3.0
Chazel et al [8]	360	94.4	73.5	37.0	4.8	97.8	87.6	80.3	1.5

Table 4.10: Comparison of classification results at sampling rate of 360 Hz

We have also reported and compared the results of the classification tasks with state of art methods in table 4.10. Columns 1 indicates the methodology used; column 2 corresponds to the sampling rate; columns 3-8 indicate the gross classifier performance in terms of Acc (Accuracy), Se (Sensitivity), PPV (Positive predictive value) and FPR (False positive rate). Row 1 reports the overall classification accuracy result using Feature Set1 and LCKSVD. The independent performance assessment of this configuration resulted in an accuracy of 93.64%, a sensitivity of 75.34%, a positive predictivity of 33.78%, and an FPR of 5.66% for the SVEB class. For the VEB class, the accuracy was 93.62% , the sensitivity was 84.66%, the positive predictivity was 50.52%, and the FPR was 5.75%. These results give competitive performance as compared to previously reported results for automated heartbeat classification systems in [6] and [8] .

We also conducted the analysis using LCKSD algorithm at a lower sampling rate and have reported the classification results in tables 4.11 - 4.17. Similar to previous results, table 4.11 and table 4.13 represent the classification performance per recording at 114Hz using Feature Set 1 - LCKSVD and using Feature Set2 - LCKSVD respectively. On the other hand, table 4.12 and table 4.14 represents the per class classification performance at 114Hz for each defined AAMI class using Feature Set 1 - LCKSVD and using Feature Set2 - LCKSVD respectively. The predicted per class classification results using algorithm FS1 - LCKSVD and FS2 - LCKSVD in table 4.12 and table 4.14 are reported in percentile (%) in table 4.15 and 4.16.

The gross classification performance per class table indicates the number of classes that are misclassified. In table 4.12, 2444 normal (N) beats were misclassified as SVEB (S) beats, and, 1147 N beats were misclassified as fusion (F) beats. Likewise in table 4.14, 1975 normal (N) beats were misclassifed as SVEB (S) beats, and, 404 N beats were misclassified as fusion (F) beats. As compared to results in [44], the number of misclassified heartbeats have decreased. However the reference paper [44] did not include per record classification results so as to compare our results with. Tables 4.17 and 4.18 illustrate the accuracy over the 5 remapped classes using FS1 and LCKSVD and FS2 and LCKSVD methodology at sampling rate of 360 Hz.

Comprehensively, the results do demonstrate that discriminative dictionary learning are better suited for the detection of VEB and SVEB type arrhythmia at lower sampling rate. Also, increasing the sampling rate to 360 Hz did not produce significant gain in performance. It therefore follows that a sampling rate of 114 Hz was found to provide enough discriminatory power for the classification task. It was observed that varying the sampling rate had minimal impact on the performance and it can be deduced that our approach emulated the performance of the state of the art models at a lower sampling rate and a set of simple features.

Record number	Beats Belonging to Class N	Beats Belonging to Class S	Beats Belonging to Class V	Beats Belonging to Class F	Beats Belonging to Class Q	Total Beats in Each Record
100	2265	1	7	0	0	2273
103	2072	5	4	3	0	2084
105	1084	1253	125	110	0	2572
111	2103	3	18	0	0	2124
113	1526	51	218	0	0	1795
117	1518	17	0	0	0	1535
121	1859	0	4	0	0	1863
123	662	824	32	0	0	1518
200	1351	634	202	414	0	2601
202	1311	297	114	414	0	2136
210	1513	728	255	154	0	2650
212	1299	1415	28	6	0	2748
213	2353	342	311	245	0	3251
214	405	541	802	514	0	2262
219	669	457	373	655	0	2154
221	853	787	407	380	0	2427
222	2076	260	128	19	0	2483
228	1696	17	310	30	0	2053
231	1559	1	10	1	0	1571
232	1403	98	276	3	0	1780
233	499	697	675	1208	0	3079
234	2653	64	7	29	0	2753

Table 4.11: Classification performance on each recording of DS2 using the AAMI recommended measures using FS1 +LCKSVD at sampling rate of 114 Hz

Reference/Algorithm	N	S	V	F	Q
N	38584	2444	2087	1144	0
S	86	1380	363	8	0
V	284	378	2448	111	0
F	334	0	20	34	0
Q	2	0	4	1	0

Table 4.12: Classification results for FS1 + LCKSVD at sampling rate of 114 Hz

We have also compared our classification results with state of art methods in Table 4.19. Columns 1 indicates the methodology used; column 2 corresponds to the sampling rate; columns 3-8 indicate the gross classifier performance in terms of Acc (Accuracy), Se (Sensitivity), PPV (Positive predictive value) and FPR (False positive

Record number	Beats Belonging to Class N	Beats Belonging to Class S	Beats Belonging to Class V	Beats Belonging to Class F	Beats Belonging to Class Q	Total Beats in Each Record
100	1049	1223	1	0	0	2273
103	1782	302	0	0	0	2084
105	2026	65	437	44	0	2572
111	2056	11	57	0	0	2124
113	1238	557	0	0	0	1795
117	308	1227	0	0	0	1535
121	1862	0	1	0	0	1863
123	1223	292	3	0	0	1518
200	1824	59	711	7	0	2601
202	1737	44	14	341	0	2136
210	2416	29	194	11	0	2650
212	2270	478	0	0	0	2748
213	2298	129	269	555	0	3251
214	532	104	1553	73	0	2262
219	1471	625	49	9	0	2154
221	1651	93	392	291	0	2427
222	1412	1061	3	7	0	2483
228	1694	55	297	7	0	2053
231	613	956	1	1	0	1571
232	1616	160	4	0	0	1780
233	1463	236	746	634	0	3079
234	2046	681	6	20	0	2753

Table 4.13: Classification performance on each recording of DS2 using the AAMI recommended measures using FS2 + LCKSVD at sampling rate of 114 Hz

Reference/Algorithm	N	S	V	F	Q
N	41535	1975	345	404	0
S	134	1265	423	15	0
V	494	130	2591	6	0
F	298	1	87	2	0
Q	4	1	2	0	0

Table 4.14: Classification results for FS2 + LCKSVD at sampling rate of 114 Hz

rate). Row 1 and 2 demonstrate the overall classification accuracy at 180Hz using Feature Set1 -LCKSVD and Feature set 2- LCKSVD respectively. Row 3 and row 4 demonstrate the overall classification accuracy at 114Hz using Feature Set1 -LCKSVD

Reference/Algorithm	N	S	V	F	Q
N	87.17%	5.52%	4.71%	2.58%	0%
S	4.68%	75.12%	19.76%	0.43%	0%
V	8.81%	11.73%	76.0%	3.44%	0%
F	86.08%	0%	5.15%	8.76%	0%
Q	28.57%	0%	57.14%	14.28%	0%

Table 4.15: Classification results in % for FS 1 + LCKSVD at sampling rate of 114Hz

Reference/Algorithm	N	S	V	F	Q
N	93.84%	4.46%	0.77%	0.91%	0%
S	7.29%	68.86%	23.02%	0.81%	0%
V	15.33%	4.03%	80.44%	0.18%	0%
F	76.80%	0.25%	22.42%	0.51%	0%
Q	57.14%	14.28%	28.57%	0%	0%

Table 4.16: Classification results in % for FS 2 + LCKSVD at sampling rate of 114Hz

and Feature set 2- LCKSVD respectively. Independent performance assessment of this configuration(i.e FS1 +LCKSVD) resulted in an accuracy of 93.4%, a sensitivity of 75.12%, a positive predictivity of 32.84%, and an FPR of 5.89% for the SVEB class. For the VEB class, accuracy was 93.51% , sensitivity was 76%, positive predictivity was 49.97%, and FPR was 5.27%. Using Feature Set 2 -LCSKVD algorithm, we obtain higher performance for both SVEB and VEB class. For the SVEB class, accuracy was 94.61% , sensitivity was 68.86%, positive predictivity was 37.52%, and FPR was 4.39% and for the VEB class, accuracy was 97.18% , sensitivity was 80.44%, positive predictivity was 70.13%, and FPR was 1.65%. These results illustrate competing performance in terms of accuracy and sensitivity when compared to previously reported results for automated heartbeat classification systems in [44]. Classification results in comparsion to the state of the art algorithm is plotted for VEB and SVEB class in Fig 4.2 and Fig 4.3 respectively. Experimental results indicate that classifiers built in this dictionary learning based framework provided competitive performance. In addition, the proposed discriminative dictionary learning algorithm opens a new window for future research, showcasing the dictionary learning based methods provide huge potential for accurate ECG data classification.

Classes	Class N	Class S	Class V	Class F	Class Q
Acc %	87.17%	93.4%	93.51%	96.74%	99.99%

Table 4.17: Accuracy for all classes using FS 1 + LCKSVD at sampling rate of 114Hz

Classes	Class N	Class S	Class V	Class F	Class Q
Acc %	92.64%	94.61%	97.18%	98.36%	99.99%

Table 4.18: Accuracy for all classes using FS 2 + LCKSVD at sampling rate of 114Hz

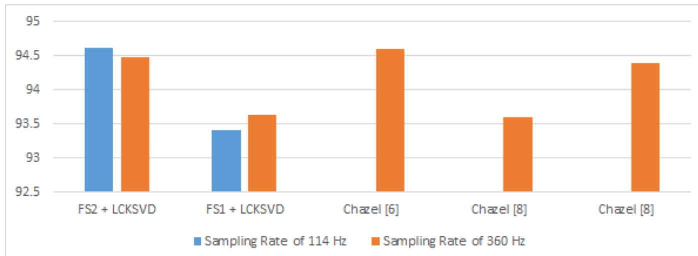

Figure 4.2: Classification results for SVEB Class

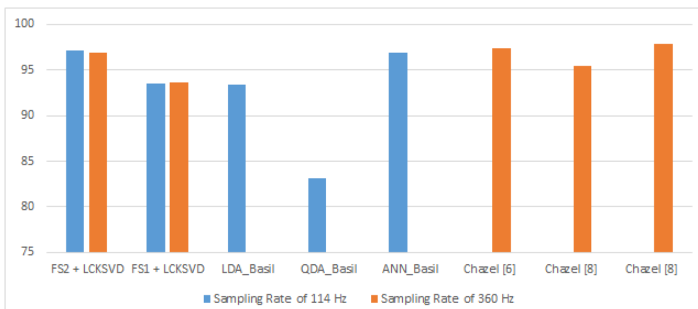

Figure 4.3: Classification results for VEB Class

Method	Rate (Hz)	SVEB				VEB			
		Acc	Se	PPV	FPR	Acc	Se	PPV	FPR
FS1+LCKSVD	180	93.17	77.57	32.33	6.22	93.04	73.8	47.65	5.62
FS2+LCKSVD	180	94.68	64.07	37.22	4.14	96.81	78.85	73.79	1.94
FS1+LCKSVD	114	93.4	75.12	32.84	5.89	93.51	76	49.97	5.27
FS2+LCKSVD	114	94.61	68.86	37.52	4.39	97.18	80.44	70.13	1.65
LDA_Basil [44]	114	-	-	-	-	93.4	75.8	61.9	4.8
QDA_Basil [44]	114	-	-	-	-	83.1	97	35.2	18.4
ANN_Basil [44]	114	-	-	-	-	96.9	79.7	74.6	1.9

Table 4.19: Comparsion of classification results for LCKSVD at sampling rate of 180 and 114 Hz

Chapter 5

CONCLUSION

Experimental results indicate that classifiers built using this dictionary learning approach demonstrate a classification accuracy of 94.61% for Supra Ventricular Ectopic Beats (SVEB) class and 97.18% for Ventricular Ectopic Beats (VEB) class at sampling rate of 114 Hz on MIT-BIH database. The dictionary learning learning based framework provided emulous performance as compared to the state of the art methods. Also, a sampling rate of 114 Hz was found to provide enough discriminatory power for the classification task. In short, our approach emulated the performance of the state of the art models at a lower sampling rate and a set of simple features. In addition, the proposed discriminative dictionary learning algorithm opens a new window for future research, showcasing the dictionary learning based methods provide huge potential for accurate ECG data classification. Future work would be to examine other types of embedding to represent the ECG recordings to serve as a feature vector and combination of better dictionary learning algorithms for robust performance.

BIBLIOGRAPHY

[1] A. Guyton and J. Hall, "11th textbook of medical physiology," 2006.

[2] "ACC/AHA clinical competence statement on electrocardiography and ambulatory electrocardiography," *Journal of the American College of Cardiology*, vol. 38, no. 7, pp. 2091–2100, 2001.

[3] L. Glass, "Cardiac oscillations and arrhythmia analysis," in *Complex Systems Science in Biomedicine*. Springer, 2006, pp. 409–422.

[4] J. Yang, K. Yu, Y. Gong, and T. Huang, "Linear spatial pyramid matching using sparse coding for image classification," in *IEEE Conference on Computer Vision and Pattern Recognition (CVPR)*, 2009, pp. 1794–1801.

[5] J. Wright, A. Y. Yang, A. Ganesh, S. S. Sastry, and Y. Ma, "Robust face recognition via sparse representation," *IEEE Transactions on Pattern Analysis and Machine Intelligence*, vol. 31, no. 2, pp. 210–227, 2009.

[6] P. De Chazal, M. O'Dwyer, and R. B. Reilly, "Automatic classification of heartbeats using ECG morphology and heartbeat interval features," *IEEE Transactions on Biomedical Engineering*, vol. 51, no. 7, pp. 1196–1206, 2004.

[7] P. de Chazal and R. B. Reilly, "A patient-adapting heartbeat classifier using ECG morphology and heartbeat interval features," *IEEE Transactions on Biomedical Engineering*, vol. 53, no. 12, pp. 2535–2543, 2006.

[8] P. de Chazal, "Detection of supraventricular and ventricular ectopic beats using a single lead ECG," in *35th Annual International Conference of IEEE Engineering in Medicine and Biology Society (EMBC)*, 2013, pp. 45–48.

[9] M. Llamedo and J. P. Martínez, "Heartbeat classification using feature selection driven by database generalization criteria," *IEEE Transactions on Biomedical Engineering*, vol. 58, no. 3, pp. 616–625, 2011.

[10] C. Ye, B. V. Kumar, and M. T. Coimbra, "Heartbeat classification using morphological and dynamic features of ECG signals," *IEEE Transactions on Biomedical Engineering*, vol. 59, no. 10, pp. 2930–2941, 2012.

[11] M. Lagerholm, C. Peterson, G. Braccini, L. Edenbrandt, and L. Sornmo, "Clustering ECG complexes using hermite functions and self-organizing maps," *IEEE Transactions on Biomedical Engineering*, vol. 47, no. 7, pp. 838–848, 2000.

[12] T. Ince, S. Kiranyaz, and M. Gabbouj, "A generic and robust system for automated patient-specific classification of ECG signals," *IEEE Transactions on Biomedical Engineering*, vol. 56, no. 5, pp. 1415–1426, 2009.

[13] X. Jiang, L. Zhang, Q. Zhao, and S. Albayrak, "ECG arrhythmias recognition system based on independent component analysis feature extraction," in *IEEE TENCON Region Conference*, 2006, pp. 1–4.

[14] L. Senhadji, G. Carrault, J. Bellanger, and G. Passariello, "Comparing wavelet transforms for recognizing cardiac patterns," *IEEE Engineering in Medicine and Biology Magazine*, vol. 14, no. 2, pp. 167–173, 1995.

[15] Y. H. Hu, S. Palreddy, and W. J. Tompkins, "A patient-adaptable ECG beat classifier using a mixture of experts approach," *IEEE Transactions on Biomedical Engineering*, vol. 44, no. 9, pp. 891–900, 1997.

[16] M. Lagerholm, C. Peterson, G. Braccini, L. Edenbrandt, and L. Sornmo, "Clustering ECG complexes using hermite functions and self-organizing maps," *IEEE Transactions on Biomedical Engineering*, vol. 47, no. 7, pp. 838–848, 2000.

[17] S. Osowski and T. H. Linh, "ECG beat recognition using fuzzy hybrid neural network," *IEEE Transactions on Biomedical Engineering*, vol. 48, no. 11, pp. 1265–1271, 2001.

[18] S. Osowski, L. T. Hoai, and T. Markiewicz, "Support vector machine-based expert system for reliable heartbeat recognition," *IEEE Transactions on Biomedical Engineering*, vol. 51, no. 4, pp. 582–589, 2004.

[19] G. de Lannoy, D. François, J. Delbeke, and M. Verleysen, "Weighted conditional random fields for supervised interpatient heartbeat classification," *IEEE Transactions on Biomedical Engineering*, vol. 59, no. 1, pp. 241–247, 2012.

[20] J. Rodriguez, A. Goni, and A. Illarramendi, "Real-time classification of ECGs on a PDA," *IEEE Transactions on Information Technology in Biomedicine*, vol. 9, no. 1, pp. 23–34, 2005.

[21] I. Christov, I. Jekova, and G. Bortolan, "Premature ventricular contraction classification by the kth nearest-neighbours rule," *Physiological measurement*, vol. 26, no. 1, p. 123, 2005.

[22] W. Jiang and S. G. Kong, "Block-based neural networks for personalized ECG signal classification," *IEEE Transactions on Neural Networks*, vol. 18, no. 6, pp. 1750–1761, 2007.

[23] J. Wiens and J. V. Guttag, "Active learning applied to patient-adaptive heartbeat classification," in *Advances in neural information processing systems*, 2010, pp. 2442–2450.

[24] Z. Jiang, Z. Lin, and L. S. Davis, "Learning a discriminative dictionary for sparse coding via label consistent K-SVD," in *IEEE Conference on Computer Vision and Pattern Recognition (CVPR)*, 2011, pp. 1697–1704.

[25] M. Elad and M. Aharon, "Image denoising via sparse and redundant representations over learned dictionaries," *IEEE Transactions on Image Processing*, vol. 15, no. 12, pp. 3736–3745, 2006.

[26] J. Mairal, F. Bach, J. Ponce, and G. Sapiro, "Online learning for matrix factorization and sparse coding," *The Journal of Machine Learning Research*, vol. 11, pp. 19–60, 2010.

[27] C. Poultney, S. Chopra, Y. L. Cun *et al.*, "Efficient learning of sparse representations with an energy-based model," in *Advances in neural information processing systems*, 2006, pp. 1137–1144.

[28] M. Aharon, M. Elad, and A. Bruckstein, "K-SVD: An algorithm for designing overcomplete dictionaries for sparse representation," *IEEE Transactions on Signal Processing*, vol. 54, no. 11, pp. 4311–4322, 2006.

[29] M. I. Owis, A. H. Abou-Zied, A. Youssef, and Y. M. Kadah, "Study of features based on nonlinear dynamical modeling in ECG arrhythmia detection and classification," *IEEE Transactions on Biomedical Engineering*, vol. 49, no. 7, pp. 733–736, 2002.

[30] K. Engan, S. O. Aase, and J. Husoy, "Frame based signal compression using method of optimal directions MOD," in *1999 IEEE International Symposium on Circuits and System (ISCAS)*, vol. 4, 1999, pp. 1–4.

[31] Q. Zhang and B. Li, "Discriminative K-SVD for dictionary learning in face recognition," in *IEEE Conference on Computer Vision and Pattern Recognition (CVPR)*, 2010, pp. 2691–2698.

[32] K. Kavukcuoglu, M. Ranzato, R. Fergus, and Y. Le-Cun, "Learning invariant features through topographic filter maps," in *IEEE Conference on Computer Vision and Pattern Recognition(CVPR)*. IEEE, 2009, pp. 1605–1612.

[33] J. Mairal, F. Bach, and J. Ponce, "Task-driven dictionary learning," *IEEE Transactions on Pattern Analysis and Machine Intelligence*, vol. 34, no. 4, pp. 791–804, 2012.

[34] M. Yang, D. Zhang, and X. Feng, "Fisher discrimination dictionary learning for sparse representation," in *International Conference on Computer Vision (ICCV)*, 2011, pp. 543–550.

[35] D.-S. Pham and S. Venkatesh, "Joint learning and dictionary construction for pattern recognition," in *IEEE Conference on Computer Vision and Pattern Recognition CVPR*, 2008, pp. 1–8.

[36] A. Atkielski, "Electrocardiogram sinus rhythm labels - wikimedia commons, http://commons.wikimedia.org/wiki/file%3asinusrhythmlabels.svg," Online accessed 20-April-2015.

[37] ""Life in the fast lane - ECG basics, http://lifeinthefastlane.com/ecg-library/basics/," Online accessed 20-April-2015.

[38] R. Mark and G. Moody, "MIT-BIH arrhythmia database," *3rd Edition*, 1997.

[39] "Electrocardiogram (ECG) Intervals, http://upload.wikimedia.org/wikipedia/commons/thumb/8/8b/ecg_intervals.svg/1280px-ecg_intervals.svg.png," Online accessed 20-April-2015.

[40] J. Mairal, J. Ponce, G. Sapiro, A. Zisserman, and F. R. Bach, "Supervised dictionary learning," in *Advances in neural information processing systems*, 2009, pp. 1033–1040.

[41] J. Yang, K. Yu, and T. Huang, "Supervised translation-invariant sparse coding," in *IEEE Conference on Computer Vision and Pattern Recognition (CVPR)*, 2010, pp. 3517–3524.

[42] J. Mairal, M. Leordeanu, F. Bach, M. Hebert, and J. Ponce, "Discriminative sparse image models for class-specific edge detection and image interpretation," in *Computer Vision–ECCV 2008*. Springer, 2008, pp. 43–56.

[43] K. Huang and S. Aviyente, "Sparse representation for signal classification," in *Advances in neural information processing systems*, 2006, pp. 609–616.

[44] T. Basil, B. S. Chandra, and C. Lakshminarayan, "A comparison of statistical machine learning methods in heartbeat detection and classification," in *Big Data Analytics*. Springer, 2012, pp. 16–25.